research papers

Mg$_{1+x}$Ir$_{1-x}$ (x = 0, 0.037 and 0.054), a binary intermetallic compound with a new orthorhombic structure type determined from powder and single-crystal X-ray diffraction

Radovan Černý,[a]* Guillaume Renaudin,[a] Vincent Favre-Nicolin,[b] Viktor Hlukhyy[c] and Rainer Pöttgen[c]

[a]University of Geneva, 24 quai Ernest-Ansermet, CH-1211 Geneva 4, Switzerland, [b]CEA/Grenoble, 17 rue des Martyrs, F-38054 Grenoble CEDEX 9, France, and [c]Institut für Anorganische und Analytische Chemie, Universität Münster, Wilhelm–Klemm–Strasse 8, D-48149 Münster, Germany

Correspondence e-mail:
radovan.cerny@cryst.unige.ch

The new binary compound Mg$_{1+x}$Ir$_{1-x}$ (x = 0–0.054) was prepared by melting the elements in the Mg:Ir ratio 2:3 in a sealed tantalum tube under an argon atmosphere in an induction furnace (single crystals) or by annealing cold-pressed pellets of the starting composition Mg:Ir 1:1 in an autoclave under an argon atmosphere (powder sample). The structure was independently solved from high-resolution synchrotron powder and single-crystal X-ray data: Pearson symbol oC304, space group *Cmca*, lattice parameters from synchrotron powder data a = 18.46948 (6), b = 16.17450 (5), c = 16.82131 (5) Å. Mg$_{1+x}$Ir$_{1-x}$ is a topologically close-packed phase, containing 13 Ir and 12 Mg atoms in the asymmetric unit, and has a narrow homogeneity range. Nearly all the atoms have Frank–Kasper-related coordination polyhedra, with the exception of two Ir atoms, and this compound contains the shortest Ir—Ir distances ever observed. The solution of a rather complex crystal structure from powder diffraction, which was fully confirmed by the single-crystal method, shows the power of powder diffraction in combination with the high-resolution data and the global optimization method.

1. Introduction

In the Mg–Ir phase diagram (Massalski *et al.*, 1996) only the composition interval of 0–25 at % Ir is reported. The intermetallic compounds with characterized crystal structures are: Mg$_{29}$Ir$_4$ (Bonhomme & Yvon, 1995), Mg$_{44}$Ir$_7$ (Westin, 1971) and Mg$_3$Ir (Range & Hafner, 1993). The compound Mg$_4$Ir is also reported (Ferro *et al.*, 1962). Our recent studies revealed that this last compound is most likely rhombohedral Mg$_{13}$Ir$_3$ (Hlukhyy, Rodewald *et al.*, 2004). Nothing is reported about compounds with higher iridium content. Recently, a new compound with the composition Mg$_5$Ir$_2$ (28.6 at % Ir) was reported (Černý *et al.*, 2002) and found to crystallize with the hexagonal Al$_5$Co$_2$-type structure [*P*6$_3$/*mmc*, a = 8.601 (1), c = 8.145 (1) Å]. Among the phases with an equiatomic composition in the Mg–*T* systems (*T* = transition metal of the VIIIth subgroup) two phases are reported with the CsCl-type structure: MgRh (Compton, 1958) and MgPd (Ferro, 1959); and MgCo (Yoshida *et al.*, 1993) with the CdNi-type structure (a substitution variant of the Ti$_2$Ni type).

An equiatomic compound with iridium as the transition metal component has not been reported. Very recently our two groups independently discovered Mg$_{1+x}$Ir$_{1-x}$ (while searching for new ternary compounds) and we characterized

Table 1
Data collection parameters and treatment for single crystals and a powder sample of $Mg_{1+x}Ir_{1-x}$.

	Single crystals	
	Crystal (1)	Crystal (2)
Formula	$Mg_{0.988+x}Ir_{1-x}$, $x = 0.037$ (1)	$Mg_{1+x}Ir_{1-x}$, $x = 0.054$(1)
Molar mass (g mol^{-1})	207.83	207.67
Space group	$Cmca$	$Cmca$
a (Å)	18.505 (4)	18.525 (4)
b (Å)	16.191 (3)	16.204 (3)
c (Å)	16.801 (3)	16.801 (3)
V (Å^3)	5034 (2)	5043 (2)
Z	152	152
Wavelength	0.71073 (Mo $K\alpha$)	0.71073 (Mo $K\alpha$)
μ (mm^{-1})	95.3	95.0
Crystal size (mm)	$0.090 \times 0.060 \times 0.045$	$0.040 \times 0.035 \times 0.030$
Absorption correction	Numerical from crystal shape and size	Numerical from crystal shape and size
Transmission ratio (max/min)	4.31	2.88
Density (calc.) (g cm^{-3})	10.42	10.39
Data collection	Stoe IPDS II	STOE IPDS II
Detector distance (mm)	60	80
Exposure time (min)	20	20
ω range; increment (°)	0–180; 1.0	0–180; 1.0
2θ interval (°)	2–33	2–32
Range in hkl	±27; ±21; ±25	±27; ±24; ±25
No. of measured reflections	30 057	29 868
No. of unique reflections	4211	4424
R_{int}	0.125	0.130
Reflections with $I > 2\sigma(I)$	3297 ($R_{sigma} = 0.0613$)	3066 ($R_{sigma} = 0.0779$)
Data/parameters	4211/190	4424/189
Structure solution	$SHELXS$97 (Sheldrick, 1997a)	$SHELXS$97 (Sheldrick, 1997a)
Structure refinement	$SHELXL$97 (Sheldrick, 1997b)	$SHELXL$97 (Sheldrick, 1997b)
S	1.089	1.007
R_F (all reflections)	0.070	0.086
$R_{wF}{}^2$ (all reflections)	0.110	0.086
Extinction coefficient	0.000030 (3)	0.000031 (2)
Residual in difference electron-density map	-5.96, 4.91	-3.58, 3.74

	Powder
Formula	MgIr
Molar mass (g mol^{-1})	216.51
Space group	$Cmca$
a (Å)	18.46948 (6)
b (Å)	16.17450 (5)
c (Å)	16.82131 (5)
V (Å^3)	5025.11 (3)
Z	152
Wavelength	0.50012
μ (mm^{-1})	3.55
Glass capillary diameter (mm)	0.2
Absorption correction	Analytical for cyclindrical shape
Density(calc.) (g cm^{-3})	10.95
Data collection	SNBL powder diffractometer
2θ step (°)	0.0025
Time/step (s)	2–7
2θ interval (°)	2.215–41.890
Min. d_{hkl} (Å)	0.6995
No. of measured reflections	3963
Reflections effectively independent (separated by more than 0.5 FWHM)	754
Durbin–Watson d statistics (Hill & Flack,1987): observed/expected	0.46/1.96
Data/parameters	754/70
Structure solution	FOX (Favre-Nicolin & Černý, 2002)
Structure refinement	$Fullprof$.2k (Rodríguez-Carvajal, 2002)
χ^2	3.02
R_{wp} (background corrected)	0.094
R_B (all reflections)	0.056
Extinction coefficient	No correction

the crystal structure of this intermetallic independently on the basis of powder and single-crystal diffraction. In the Geneva group $Mg_{1+x}Ir_{1-x}$ was first obtained in the mixture with Mg_3Ir and MgO by annealing the powder sample of the complex hydride $Mg_6Ir_2H_{11}$ (Černý et al., 2002; Kohlmann, 1999) at 1300 K for 16 d. A single-phase powder sample was further prepared from elemental powders and structurally characterized by synchrotron powder diffraction. The Münster group investigated the ternary system Mg–In–Ir with respect to the extended solid solutions $Mg_{3-x}In_xIr$, $In_{2-x}Mg_xIr$ (Hlukhyy, Hoffmann & Pöttgen, 2004a), $In_{3-x}Mg_xIr$ (Hlukhyy, Hoffmann & Pöttgen, 2004b) and $Mg_{13-x}In_xIr_3$ (Hlukhyy & Pöttgen, 2004a) of the binaries Mg_3Ir, In_2Ir, In_3Ir and $Mg_{13}Ir_3$ (Hlukhyy, Rodewald et al., 2004). The first indicators of the $Mg_{1+x}Ir_{1-x}$ structure came from the ternary samples. Single crystals were then grown from binary samples. The independent characterization of the compound by two groups allows the possibility of comparing the results obtained by the powder and single-crystal diffraction methods on a relatively complex crystal structure. Herein we report on the synthesis and structural elucidation of this new binary magnesium compound $Mg_{1+x}Ir_{1-x}$.

2. Experimental and results

2.1. Synthesis

2.1.1. Sample for powder diffraction. The successful synthesis of polycrystalline $Mg_{1+x}Ir_{1-x}$ was achieved by sintering powders of the elements. A stoichiometric mixture of Mg (Cerac, 99.6%, -400 mesh) and Ir powder (Alfa Aesar, 99.9%, -325 mesh) was compressed into pellets of ca 1 g and placed in an autoclave filled with 1 bar of argon at room temperature. The temperature was increased to 673 K within 1 d and then to 873 K within 2 d and then the sample was slowly cooled over 6 h to

	Powder
Effective multiplier SCOR for the uncertainties of structural parameters:	
Bérar & Lelann (1991)	3.78
Pawley (1980)	4.44

room temperature. No weight losses were observed after the annealing procedure. Careful inspection of the black bulk samples obtained has shown the absence of single crystals. The bulk sample was powdered under a protective argon atmosphere, although the $Mg_{1+x}Ir_{1-x}$ phase is stable in air. Laboratory X-ray powder diffraction data showed that the sample contained binary $Mg_{1+x}Ir_{1-x}$ and a small amount of iridium metal. The composition of the alloy was measured on the powder sample with EDX using the standard method and MgK and IrM edges. The average composition obtained from ten points is $Mg_{52\,(2)}Ir_{48\,(2)}$. The scatter of the results from the ten measurements was low, indicating that they correspond to the same phase and are not influenced by the impurity phase.

2.1.2. Sample for single-crystal diffraction. The starting materials for the preparation of the samples used for crystal growth were a magnesium rod (Johnson Matthey, Ø 16 mm, > 99.5%) and iridium powder (Degussa-Hüls, 200 mesh, > 99.9%). Pieces of the magnesium rod (the surface of the rod was first cut on a turning lathe in order to remove surface impurities) and a cold-pressed pellet of iridium (Ø 6 mm) were weighed in the atomic ratio Mg:Ir 2:3 (well shaped single crystals were only obtained with an excess of iridium, while the samples with a 1:1 starting composition remained polycrystalline) and the mixture was sealed in a tantalum tube (Pöttgen *et al.*, 1999). The ampoule was placed in a water-cooled sample chamber (Kußmann *et al.*, 1998) of an induction furnace (Hüttinger Elektronik, Freiburg, Typ TIG 1.5/300) and heated under flowing argon up to ∼1400 K. The argon was purified over silica gel, molecular sieves and titanium sponge (900 K). After the melting procedure the sample was cooled within 30 min to ∼ 1300 K and held at that temperature for another 30 min. Then the sample was cooled within 90 min to ∼ 700 K and finally quenched by switching off the furnace. The light gray sample could easily be separated from the tantalum tube. No reactions whatsoever of the sample with the crucible material could be detected. $Mg_{1+x}Ir_{1-x}$ is stable in moist air as a compact button as well as a fine-grained powder. Single crystals exhibit metallic luster.

The compact sample and the single crystals investigated have been analyzed by an EDX measurement using a LEICA 420 I scanning electron microscope with MgO and iridium as standards. No impurity elements were detected. For the analyses of the bulk sample, irregularly shaped pieces were embedded in a methacrylate matrix, polished and then examined in the scanning electron microscope in the back-scattering mode. The various analyses revealed the composition of the main phase as $Mg_{52\,(1)}Ir_{48\,(1)}$, with elemental iridium as a secondary phase.

2.2. Diffraction

2.2.1. Powder diffraction. Synchrotron powder diffraction data were obtained at the Swiss–Norwegian Beam Line (SNBL) at the ESRF Grenoble (the sample was placed in a glass capillary) with a six-analyser crystals detector. Details of the data collection are given in Table 1.[1]

2.2.2. Single-crystal diffraction. The bulk sample from the crystal growth experiments has been characterized through its Guinier powder pattern. The Guinier camera was equipped with an image plate system (Fujifilm, BAS-1800) and monochromated Cu $K\alpha_1$ radiation. α-Quartz (a = 4.9130, c = 5.4046 Å) was used as an internal standard. The orthorhombic lattice parameters were obtained from least-squares fits of the powder data. The correct indexing of the pattern was ensured by an intensity calculation (Yvon *et al.*, 1977), taking the atomic positions from the structure refinement. The powder lattice parameters of the bulk sample, a = 18.513 (3), b = 16.201 (3), c = 16.799 (4) Å, V = 5038.7 Å^3, are between the values obtained from the two single crystals (Table 1) and overlap with them within the combined standard deviations. As is evident from the starting composition, the X-ray powder pattern and the EDX data revealed elemental iridium as a second phase.

Small, irregularly shaped single crystals of the inductively melted sample were obtained by mechanical fragmentation of the same bulk sample. These crystals were first examined by the use of a Buerger camera equipped with an image plate system (Fujifilm BAS–1800) in order to establish suitability for intensity data collection. Single-crystal intensity data were collected at room temperature by the use of a Stoe IPDS II image plate diffractometer. All the relevant details concerning the data collections are listed in Table 1.

2.3. Structure solution and refinement

2.3.1. Powder diffraction. The crystal structure of $Mg_{1+x}Ir_{1-x}$ was solved and refined using the synchrotron diffraction data. No known phase from the Mg–Ir system was identified in the observed synchrotron powder pattern. Therefore, the first 26 observed reflections were used for indexing the unknown pattern using the program *DICVOL*91 (Boultif & Louër, 1991). An orthorhombic cell was found with figures-of-merit M = 13.2 and F = 108.0. The refined values of the lattice parameters from a final Rietveld refinement are given in Table 1. From the analysis of the powder pattern the extinction symbol C-$c(ab)$ was determined, corresponding to the space groups $C2cb$(41) and $Cmca$(64). The centrosymmetric group $Cmca$ was used for the structure solution.

---

[1] Supplementary data for this paper are available from the IUCr electronic archives (Reference: AV5006). Services for accessing these data are described at the back of the journal.

Table 2
Atomic positional and displacement parameters for $Mg_{1+x}Ir_{1-x}$: **MgIr (powder diffraction)**, $Mg_{1+x}Ir_{1-x}$, x = 0.037 [crystal (1)], $Mg_{1+x}Ir_{1-x}$, x = 0.054 [crystal (2)].

The isotropic displacement parameter U was used for the refinement of powder diffraction data. The equivalent isotropic displacement parameter U_{eq}, defined as one third of the trace of the orthogonalized U^{ij} tensor, is given for the refinement of the single-crystal diffraction data.

	Site	x	y	z	U_{eq}/U [Å²]
Ir1	**16(g)**	**0.0668 (1)**	**0.1158 (1)**	**0.4161 (1)**	**0.01647 (6)**
		0.06690 (3)	*0.11400 (5)*	*0.41556 (3)*	*0.0062 (1)*
		0.06692 (4)	0.11394 (4)	0.41552 (4)	0.0079 (1)
Ir2	**16(g)**	**0.0689 (1)**	**0.3926 (1)**	**0.4114 (1)**	**= U_{Ir1}**
$M2$ [$M = Ir_{0.684\,(6)}Mg_{0.316\,(6)}$]		*0.06917 (5)*	*0.39291 (7)*	*0.41158 (5)*	*0.0072 (3)*
$M2$ [$M = Ir_{0.667\,(6)}Mg_{0.333\,(6)}$]		0.06922 (6)	0.39303 (6)	0.41162 (6)	0.0086 (3)
Ir3	**16(g)**	**0.07161 (8)**	**0.19842 (9)**	**0.1628 (1)**	**= U_{Ir1}**
		0.07150 (3)	*0.19825 (5)*	*0.16153 (4)*	*0.0069 (1)*
		0.07150 (3)	0.19837 (4)	0.16150 (5)	0.0084 (1)
Ir4	**16(g)**	**0.1372 (1)**	**0.1564 (1)**	**0.0411 (1)**	**= U_{Ir1}**
		0.13896 (3)	*0.15669 (5)*	*0.04101 (3)*	*0.0064 (1)*
		0.13910 (4)	0.15670 (4)	0.04100 (4)	0.0078 (1)
Ir5	**16(g)**	**0.1384 (1)**	**0.1564 (1)**	**0.2858 (1)**	**= U_{Ir1}**
		0.13747 (3)	*0.15614 (5)*	*0.28543 (3)*	*0.0062 (1)*
		0.13746 (4)	0.15607 (4)	0.28537 (4)	0.0077 (1)
Ir6	**16(g)**	**0.36484 (8)**	**0.2508 (2)**	**0.0881 (1)**	**= U_{Ir1}**
$M6$ [$M = Ir_{0.846\,(6)}Mg_{0.154\,(6)}$]		*0.36492 (4)*	*0.24932 (6)*	*0.08777 (4)*	*0.0060 (3)*
$M6$ [$M = Ir_{0.823\,(5)}Mg_{0.177\,(5)}$]		0.36477 (4)	0.24928 (5)	0.08787 (5)	0.0077 (2)
Ir7	**8(f)**	0	**0.3364 (2)**	**0.1710 (2)**	**= U_{Ir1}**
		0	*0.33535 (7)*	*0.16990 (5)*	*0.0077 (2)*
		0	0.33536 (5)	0.16992 (6)	0.0093 (2)
Ir8	**8(f)**	0	**0.4329 (2)**	**0.2813 (2)**	**= U_{Ir1}**
		0	*0.43135 (7)*	*0.28280 (5)*	*0.0077 (2)*
		0	0.43130 (6)	0.28290 (6)	0.0090 (2)
Ir9	**8(e)**	$\frac{1}{4}$	**0.0786 (2)**	$\frac{1}{4}$	**= U_{Ir1}**
		$\frac{1}{4}$	*0.07881 (7)*	$\frac{1}{4}$	*0.0071 (2)*
		$\frac{1}{4}$	0.07875 (5)	$\frac{1}{4}$	0.0088 (2)
Ir10	**8(e)**	$\frac{1}{4}$	**0.4262 (2)**	$\frac{1}{4}$	**= U_{Ir1}**
		$\frac{1}{4}$	*0.42525 (7)*	$\frac{1}{4}$	*0.0088 (2)*
		$\frac{1}{4}$	0.42521 (6)	$\frac{1}{4}$	0.0098 (2)
Ir11	**8(d)**	**0.1362 (2)**	0	0	**= U_{Ir1}**
		0.13829 (5)	0	0	*0.0085 (2)*
		0.13858 (6)	0	0	0.0097 (2)
Ir12	**8(d)**	**0.3744 (2)**	0	0	**= U_{Ir1}**
		0.37295 (5)	0	0	*0.0078 (2)*
		0.37293 (5)	0	0	0.0094 (2)
Ir13	**8(c)**	$\frac{1}{4}$	$\frac{1}{4}$	0	**= U_{Ir1}**
		$\frac{1}{4}$	$\frac{1}{4}$	0	*0.0066 (2)*
		$\frac{1}{4}$	$\frac{1}{4}$	0	0.0081 (2)
Mg1	**16(g)**	**0.1228 (8)**	**0.3301 (9)**	**0.0621 (8)**	**0.0075 (9)**
		0.1239 (4)	*0.3334 (5)*	*0.0613 (4)*	*0.010 (1)*
		0.1234 (4)	0.3323 (4)	0.0606 (4)	0.012 (1)
Mg2	**16(g)**	**0.1375 (8)**	**0.0278 (7)**	**0.161 (1)**	**= U_{Mg1}**
		0.1326 (4)	*0.0307 (5)*	*0.1636 (4)*	*0.012 (1)*
		0.1331 (4)	0.0315 (4)	0.1628 (5)	0.011 (1)
Mg3	**16(g)**	**0.1352 (7)**	**0.3375 (9)**	**0.2721 (8)**	**= U_{Mg1}**
		0.1307 (4)	*0.3331 (5)*	*0.2650 (4)*	*0.010 (1)*
		0.1308 (4)	0.3330 (4)	0.2659 (4)	0.011 (1)
Mg4	**16(g)**	**0.1235 (7)**	**0.4779 (8)**	**0.1736 (9)**	**= U_{Mg1}**
Occupancy 0.89 (4)		*0.1275 (4)*	*0.4838 (5)*	*0.1688 (4)*	*0.008 (2)*
		0.1276 (4)	0.4850 (4)	0.1692 (5)	0.013 (1)
Mg5	**16(g)**	**0.2230 (6)**	**0.2243 (7)**	**0.1678 (8)**	**= U_{Mg1}**
		0.2288 (4)	*0.2332 (5)*	*0.1660 (4)*	*0.012 (1)*
		0.2289 (4)	0.2331 (4)	0.1664 (5)	0.014 (1)
Mg6	**16(g)**	**0.2751 (8)**	**0.0874 (9)**	**0.0738 (8)**	**= U_{Mg1}**
		0.2720 (4)	*0.0894 (5)*	*0.0766 (4)*	*0.012 (1)*
		0.2721 (4)	0.0899 (4)	0.0753 (5)	0.015 (1)
Mg7	**16(g)**	**0.2657 (7)**	**0.3949 (9)**	**0.0980 (8)**	**= U_{Mg1}**
		0.2716 (4)	*0.3984 (5)*	*0.0944 (4)*	*0.014 (1)*
		0.2715 (4)	0.3992 (4)	0.0941 (5)	0.015 (1)
Mg8	**8(f)**	0	**0.065 (1)**	**0.070 (1)**	**= U_{Mg1}**
		0	*0.0638 (7)*	*0.0690 (6)*	*0.012 (2)*
		0	0.0629 (6)	0.0694 (6)	0.010 (2)
Mg9	**8(f)**	0	**0.086 (1)**	**0.265 (1)**	**= U_{Mg1}**
		0	*0.0847 (7)*	*0.2650 (5)*	*0.009 (2)*
		0	0.0849 (5)	0.2651 (5)	0.008 (2)

Attempts to solve the structure by methods using extracted integrated intensities from the powder pattern (direct methods or Patterson synthesis) failed, probably because of the difficulty in recognizing a structural motif, either in E- or Patterson maps. The structure was therefore solved by the global optimization of a structural model in direct space using the simulated annealing (in parallel tempering mode) and the recently developed program *FOX* (Favre-Nicolin & Černý, 2002). As a cost function, the integrated wR factor (Favre-Nicolin & Černý, 2002) and anti-bump function (based on the minimal distances Mg—Ir 2.7 and Mg—Mg 2.8 Å) weighted at 0.55/0.45 were used. As the crystal structure was expected to be closely packed, the expected volume per atom was estimated as 15–20 Å³. No density measurements were available and no indication of a structural relation with a known structure type was found from analysis of the cell parameters. First, we introduced 11 free Mg atoms and 11 free Ir atoms at random positions in the cell, and used the Dynamical Occupancy Correction (Favre-Nicolin & Černý, 2002) with the advantages of automatic identification of the special crystallographic positions and of merging the excess atoms. All 22 atoms were quickly localized and from 11 positions of Mg, two were identified by further occupancy optimization as being in fact occupied by Ir rather than Mg. Next, 13 already localized Ir atoms were kept fixed and the number of free Mg atoms was subsequently increased in steps of 1 until 12 Mg atoms were localized, and all the additional Mg atoms introduced into the model were systematically merged by the program. In a final run (repeated many times) 13 Ir and 12 Mg free atoms were optimized simultaneously (75 degrees of freedom), and the same solution was always found in less than 5 min (600 Mhz Pentium III computer). For the correct solution the integrated wR was 0.09 and the profile R_{wp} was 0.11.

The crystal structure of $Mg_{1+x}Ir_{1-x}$ was refined by the Rietveld method using the synchrotron data and the program *Full-Prof*.2k (Rodríguez-Carvajal, 2002). Iridium metal was identified as an impurity (2.5 wt %). Runs were performed in which the occupancies of the individual atomic sites were refined. All sites refined to full occupancy and no mixed sites were observed. In the final run 76 parameters were refined

Table 2 (continued)

	Site	x	y	z	U_{eq}/U [Å^2]
Mg10	8(*f*)	0	**0.241 (1)**	**0.004 (1)**	**$= U_{Mg1}$**
		0	*0.2410 (7)*	*0.0034 (5)*	*0.011 (2)*
		0	0.2419 (6)	0.0041 (6)	0.010 (2)
Mg11	8(*f*)	0	**0.253 (1)**	**0.328 (1)**	**$= U_{Mg1}$**
		0	*0.2509 (7)*	*0.3233 (5)*	*0.010 (2)*
		0	0.2501 (6)	0.3230 (5)	0.011 (2)
Mg12	8(*f*)	0	**0.450 (1)**	**0.061 (1)**	**$= U_{Mg1}$**
		0	*0.4526 (7)*	*0.0667 (5)*	*0.011 (2)*
		0	0.4531 (5)	0.0675 (6)	0.012 (2)

(main phase: 57 positional and 2 isotropic displacement, 3 cell, 7 pseudo-Voigt-profile functions and 1 scale; impurity: 1 displacement, 1 cell, 3 pseudo-Voigt profile functions and 1 scale). The final agreement factors are $R_{wp} = 0.094$, $\chi^2 = 3.02$, R_B (MgIr) = 0.056. The refined structural parameters are summarized in Table 2 and the Rietveld plot is shown in Fig. 1.

2.3.2. Single-crystal diffraction. Analysis of the diffractometer data sets revealed high orthorhombic Laue symmetry and *C*-centered lattices. The extinction conditions were compatible with the space group *Cmca*. The starting atomic parameters were deduced from an automatic interpretation of direct methods with *SHELXS*97 (Sheldrick, 1997*a*) and they were subsequently refined using *SHELXL*97 (Sheldrick, 1997*b*; full-matrix least-squares on F^2) with anisotropic atomic displacement parameters for all atoms. The equivalent isotropic displacement parameters for the Ir2 and Ir6 sites of both crystals showed larger values than for the other atoms, indicating a lower scattering power at these positions. In agreement with the slightly higher magnesium content derived from the EDX analyses, we refined these positions with a mixed Ir/Mg occupancy. As a check for the correct site
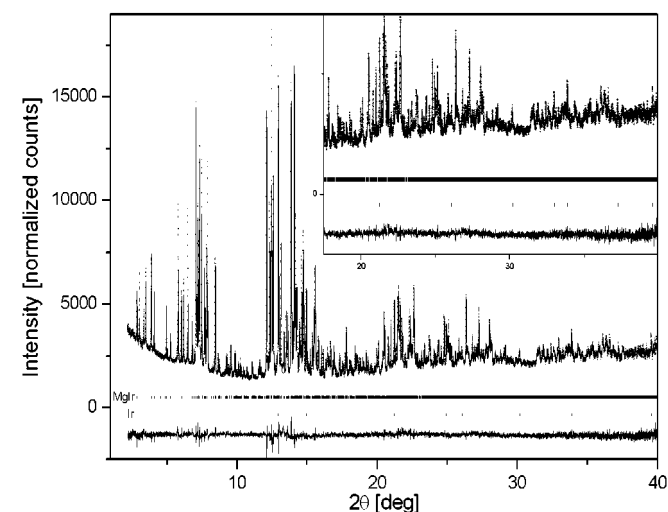
assignments, the occupancy parameters of the remaining sites were refined in separate series of least-squares cycles. Most sites were fully occupied within two standard deviations. An exception is the Mg4 site of crystal (1), which has an occupancy parameter of only 89 (4)%. Although this site is fully occupied within three standard deviations, refinement with the lower occupancy slightly improved the residuals. In the final cycles this site was refined with a free occupancy, while all other sites were refined with ideal occupancies. However, for the sake of simplicity we term the compound '$Mg_{1+x}Ir_{1-x}$' without specifying that the defect is located at the Mg4 site. The final difference-Fourier synthesis revealed no significant residual peaks (Table 1). The highest residual densities were close to the iridium sites and most likely resulted from incomplete absorption correction. The positional parameters of the refinements are listed in Table 2 and the anisotropic displacement parameters are given in Table 3. Selected interatomic distances (Å) for the single crystal (1) are given in Table 4. Listings of the observed and calculated structure factors are available.[2]

3. Discussion

3.1. Powder *versus* single-crystal results

Independent studies of $Mg_{1+x}Ir_{1-x}$ by single-crystal and powder diffraction methods have allowed the comparison of the structural results obtained by two different methods on a compound having rather a complex crystal structure with 304 atoms in the unit cell. The differences between the two methods of sample preparation prevents us from doing a more detailed comparison of both methods. We are therefore only comparing the results obtained by both methods and discussing whether both results describe the same compound. First we make a short comparison of both experiments.

The investigated volumes in reciprocal space are approximately the same in both experiments, thus giving a similar number of unique reflections: 4211 and 4424 for the single-crystal data and 3963 for the powder data. However, the equivalent reflections are measured in the single-crystal experiment independently, giving a redundancy factor of *ca* 7. Moreover, not all 3963 reflections in the powder pattern can be considered as independent observations, because of the profile overlap in the pattern. Considering as independent reflections only those that are distant at least by 0.5 FWHM from an adjacent reflection, the number of unique reflections in the powder pattern is only 754. This is still enough to have a data/parameters ratio of *ca* 10 if the displacement parameters are refined isotropically and constrained to only two values (one for Ir atoms and the other for Mg atoms). Nevertheless,

Figure 1
Rietveld plot of MgIr ($R_{wp} = 0.094$, $\chi^2 = 3.02$). Observed (dots) and calculated (solid line) synchrotron (SNBL) powder diffraction patterns ($\lambda = 0.50012$ Å) are shown with a difference curve below. The ticks indicate the line positions of the main phase MgIr ($R_B = 0.056$) and the impurity phase Ir.

[2] Details may be obtained from: Fachinformationszentrum Karlsruhe, D-76344 Eggenstein-Leopoldshafen (Germany), by quoting the Registry No's. CSD-413931 ($Mg_{1.037}Ir_{0.963}$) and CSD-413930 ($Mg_{1.054}Ir_{0.946}$).

the single-crystal data are highly superior in this comparison: the data/parameter ratio is 22–23 even if all atoms are refined independently with anisotropic displacement parameters. A more accurate evaluation of the independence of reflections in the powder pattern could be performed on the basis of the Bayesian probability approach (David, 1999). It would increase the number of independently observed reflections in the powder data maximally by 10%, because that approach evaluates the information from two reflections closer than 0.5 FWHM as being maximally 10% superior to the information from one reflection (see Fig. 5 in David, 1999).

The standard uncertainties (s.u.) of the results obtained from the single crystals will hereafter be known as σ_{sc1} and σ_{sc2} (σ_{sc} being the maximum from σ_{sc1} and σ_{sc2}) and those from the powder sample σ_{pw}. Please note that the values of all the s.u.'s given here are as they were calculated by the respective refinement programs $SHELXL$97 and $FullProf$.2k. It is, however, well known that the precision of the structural parameters is overestimated in powder diffraction owing to serial correlations in the observed data (individual points in the powder pattern) and the non-accessibility of the goodness-of-fit parameter based on the integrated intensities of individual reflections. Several theoretical models were proposed to correct this handicap, two of them are available in the program $FullProf$.2k: Bérar & Lelann (1991) and Pawley (1980). The multiplication factor SCOR for all σ_{pw}, according to these two models, is given in Table 1. The d parameter of the Durbin–Watson statistics (Hill & Flack, 1987), showing the presence of serial correlations in the powder diffraction data, is also given.

The structural results obtained from the two single crystals differ significantly only in the lattice parameters (1–5 σ_{sc}) and

in the refined composition ($17\sigma_{sc}$). The atomic positional parameters obtained from the two single crystals differ mostly within 3 σ_{sc} (95% of parameters) with the exception of the x parameter and $M6$ (4 σ_{sc}) of Ir4 and Ir11 (5 σ_{sc}). The equivalent displacement parameters U_{eq} obtained from the two single crystals differ within 3 σ_{sc} for Mg atoms, but within 5–17 σ_{sc} for Ir atoms, and they are systematically higher for crystal (2), which reflects the higher concentration of point lattice defects (vacancies, interstitial atoms) in this crystal. We conclude that the two crystals are isotypic and that they differ in chemical composition, as reflected in the occupancies of three atomic sites.

The standard uncertainties σ_{pw} of the lattice parameters are 60–66 times smaller than the corresponding σ_{sc} values. When multiplying σ_{pw} by the SCOR factor, this difference is only ca 15 times in favor of powder diffraction. It confirms, nevertheless, the higher precision of the lattice parameters determined from high-resolution synchrotron powder diffraction than those determined by X-ray single-crystal diffraction with an area detector.

The atomic positional parameters obtained from the powder sample seem to differ significantly from those obtained from the single crystals. The standard uncertainties σ_{pw} of the atomic positional parameters are two–three times higher for Ir atoms and twice as high for Mg atoms than the corresponding σ_{sc} values. Differences between the powder data and single-crystal results for the Ir atoms are within 1–18 σ_{pw}, those for Mg atoms are within 1–13 σ_{pw}. However, if we apply the multiplication factor SCOR of σ_{pw} for powder data according to the two models given in Table 1, the differences stay to within three SCOR × σ_{pw}, with few exceptions of four–five SCOR × σ_{pw}. We can conclude that the main phase of the powder sample is isotypic to that found in both single crystals.

3.2. Chemical composition

The structural results from the single crystals differ in the occupancies of three atomic sites, resulting in a slightly different chemical composition [crystal (2) contains more magnesium]. As already discussed in §2.3.1, Rietveld refinement of the occupancies of individual atomic sites has converged to a fully ordered structure within 3 σ_{pw} of the refined occupancies. The refinement with the result from crystals (1) or (2) as a starting model has also converged to a fully ordered structure within 3 σ_{pw} of the refined occupancies. As the EDX result obtained on the powder sample also shows the stoichiometric composition to be 1:1 within the precision of the EDX measurement,
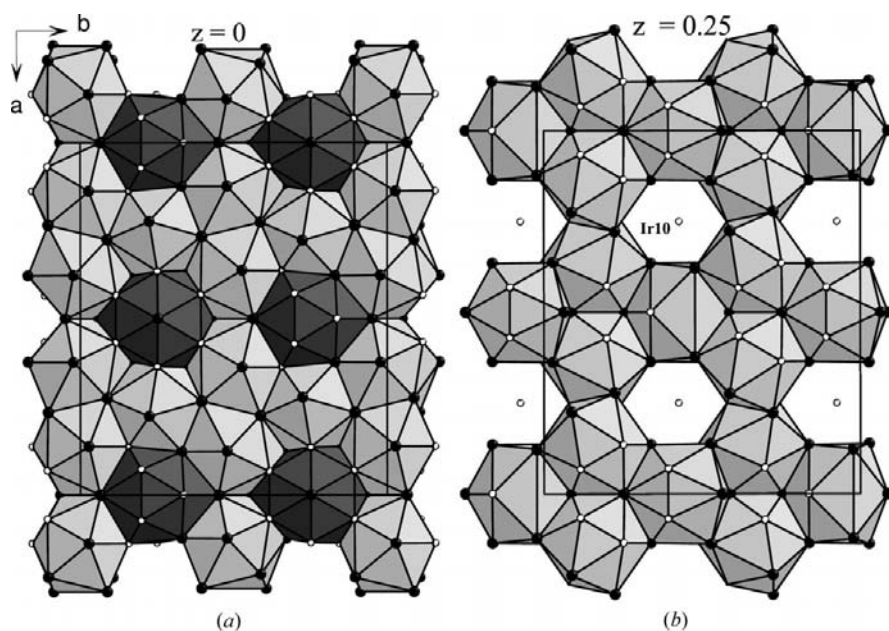
Figure 2
Structural slabs of $Mg_{1+x}Ir_{1-x}$ at (a) $z \simeq 0$, Ir11, Ir12 and Ir13 icosahedrons (light) and an Mg10 Frank–Kasper polyhedron with CN16 (dark); (b) $z \simeq 0.25$, Ir5 and Ir8 icosahedrons, and an Ir10 atom. Ligand atoms: Ir – small white spheres; Mg – large black spheres.

Table 3
Anisotropic displacement parameters (pm^2) for two single crystals of $Mg_{1+x}Ir_{1-x}$ ($x = 0.037$ and 0.054).

	Site	U^{11}	U^{22}	U^{33}	U^{23}	U^{13}	U^{12}
Crystal (1), $Mg_{1+x}Ir_{1-x}$ ($x = 0.037$)							
Ir1	16(g)	85 (3)	45 (4)	58 (2)	4 (2)	2 (2)	−5 (2)
M2	16(g)	91 (5)	44 (6)	81 (4)	−3 (3)	−10 (3)	3 (3)
Ir3	16(g)	88 (3)	61 (4)	57 (2)	2 (2)	0 (2)	−2 (2)
Ir4	16(g)	89 (3)	48 (4)	55 (2)	0 (2)	2 (2)	1 (2)
Ir5	16(g)	86 (3)	50 (4)	51 (2)	1 (2)	−3 (2)	1 (2)
M6	16(g)	91 (3)	39 (5)	50 (3)	7 (2)	−3 (2)	7 (3)
Ir7	8(f)	118 (4)	50 (5)	61 (3)	5 (3)	0	0
Ir8	8(f)	130 (4)	34 (5)	69 (3)	4 (3)	0	0
Ir9	8(e)	77 (4)	63 (5)	73 (3)	0	2 (3)	0
Ir10	8(e)	91 (4)	79 (6)	93 (3)	0	9 (3)	0
Ir11	8(d)	132 (4)	51 (5)	71 (3)	3 (3)	0	0
Ir12	8(d)	97 (4)	58 (5)	78 (3)	−23 (3)	0	0
Ir13	8(c)	79 (3)	56 (5)	64 (3)	4 (3)	−2 (3)	−5 (3)
Mg1	16(g)	152 (30)	69 (39)	85 (23)	26 (21)	27 (21)	8 (23)
Mg2	16(g)	174 (30)	87 (39)	103 (24)	−3 (23)	−27 (23)	31 (24)
Mg3	16(g)	99 (26)	77 (39)	118 (24)	−2 (23)	−16 (20)	13 (22)
Mg4	16(g)	154 (37)	26 (45)	64 (30)	−19 (22)	13 (23)	39 (24)
Mg5	16(g)	93 (25)	183 (42)	90 (24)	20 (23)	11 (20)	42 (23)
Mg6	16(g)	130 (29)	126 (43)	112 (25)	29 (23)	11 (22)	3 (25)
Mg7	16(g)	151 (30)	143 (45)	129 (27)	−32 (24)	34 (23)	−35 (26)
Mg8	8(f)	139 (41)	38 (56)	174 (40)	−23 (33)	0	0
Mg9	8(f)	101 (37)	63 (53)	106 (34)	27 (30)	0	0
Mg10	8(f)	117 (37)	86 (55)	112 (35)	−21 (32)	0	0
Mg11	8(f)	129 (38)	44 (51)	113 (33)	5 (30)	0	0
Mg12	8(f)	113 (39)	89 (57)	114 (36)	−54 (32)	0	0
Crystal (2), $Mg_{1+x}Ir_{1-x}$ ($x = 0.054$)							
Ir1	16(g)	75 (3)	88 (3)	74 (3)	5 (2)	3 (2)	−6 (2)
M2	16(g)	78 (5)	85 (5)	96 (6)	2 (3)	−13 (3)	0 (3)
Ir3	16(g)	77 (3)	100 (2)	74 (3)	3 (2)	−2 (3)	4 (2)
Ir4	16(g)	75 (3)	90 (2)	68 (3)	1 (2)	3 (2)	−1 (2)
Ir5	16(g)	74 (3)	89 (2)	67 (3)	−3 (2)	5 (2)	0 (2)
M6	16(g)	75 (3)	82 (3)	74 (4)	10 (2)	−5 (3)	3 (3)
Ir7	8(f)	111 (4)	90 (3)	77 (4)	7 (3)	0	0
Ir8	8(f)	113 (4)	80 (4)	79 (4)	4 (3)	0	0
Ir9	8(e)	70 (4)	100 (4)	94 (4)	0	−1 (4)	0
Ir10	8(e)	73 (4)	119 (4)	102 (4)	0	6 (4)	0
Ir11	8(d)	123 (4)	84 (3)	85 (4)	6 (3)	0	0
Ir12	8(d)	87 (4)	97 (3)	97 (4)	−23 (3)	0	0
Ir13	8(c)	65 (3)	98 (3)	80 (4)	3 (3)	0 (4)	−10 (3)
Mg1	16(g)	90 (29)	170 (29)	86 (30)	6 (23)	−25 (25)	−30 (21)
Mg2	16(g)	96 (27)	172 (27)	75 (28)	−18 (26)	29 (28)	47 (21)
Mg3	16(g)	108 (29)	129 (27)	92 (30)	38 (22)	−2 (24)	13 (21)
Mg4	16(g)	135 (30)	105 (26)	145 (33)	−53 (23)	−9 (28)	4 (20)
Mg5	16(g)	136 (29)	161 (29)	131 (32)	4 (25)	35 (29)	68 (21)
Mg6	16(g)	99 (31)	176 (31)	177 (37)	7 (26)	19 (30)	11 (23)
Mg7	16(g)	154 (34)	142 (30)	145 (35)	−42 (24)	54 (28)	−39 (24)
Mg8	8(f)	88 (39)	114 (37)	103 (44)	12 (32)	0	0
Mg9	8(f)	65 (37)	163 (39)	9 (39)	−34 (29)	0	0
Mg10	8(f)	40 (32)	211 (41)	58 (37)	9 (36)	0	0
Mg11	8(f)	131 (38)	131 (34)	55 (38)	−27 (32)	0	0
Mg12	8(f)	113 (42)	95 (36)	147 (48)	40 (32)	0	0

the synthesis: quenching from 700 K for single crystals and slow cooling from 873 K for the powder sample. It indicates that the narrow homogeneity range only exists at higher temperatures.

3.3. Crystal chemistry – atomic coordination

Binary $Mg_{1+x}Ir_{1-x}$ crystallizes with a peculiar new orthorhombic structure type, with the space group *Cmca* and Pearson's symbol oC304 (Pearson, 1967). The compound contains 13 crystallographically independent iridium and 12 independent magnesium sites, shows a small homogeneity range observed as two mixed iridium–magnesium sites (Ir2 and Ir6, listed as *M* in Table 2), and can be defective as observed by one partly occupied magnesium site on the single crystal (1). At first sight the coordination polyhedra and the course of the interatomic distances for the mixed sites are not peculiar. In the review of coordination polyhedra given below these sites are considered as iridium sites.

$Mg_{1+x}Ir_{1-x}$ can be classified as a topologically close-packed phase that mostly follows the definition of Frank–Kasper phases (Frank & Kasper, 1958, 1959) as the coordination of nearly all the atoms has a form of Frank–Kasper polyhedra. Most of the Ir atoms are coordinated by the icosahedra: Ir2, Ir4, Ir6 by Mg_7Ir_5; Ir1, Ir3, Ir5, Ir11, Ir13 by Mg_8Ir_4; Ir7, Ir8 by Mg_9Ir_3 and Ir12 by $Mg_{10}Ir_2$. Two Ir atoms are coordinated by a polyhedron with CN 11: Ir9 by Mg_8Ir_3 and Ir10 by $Mg_{10}Ir_1$. All Mg atoms are coordinated by Frank–Kasper polyhedra with CN 14, 15 or 16: Mg1, Mg3, Mg4, Mg7, Mg9, Mg12 by Mg_7Ir_7; Mg6 by Mg_6Ir_8; Mg2, Mg5 by Mg_7Ir_8; Mg8, Mg10 by Mg_5Ir_{11} and Mg11 by Mg_4Ir_{12}.

3.4. Structure topology and relation with other phases

It is quite difficult to relate the $Mg_{1+x}Ir_{1-x}$ crystal structure to structures of other known intermetallic compounds. However, the structure can be rationalized as a stacking of (001) slabs at $z \simeq 0$ and $\frac{1}{2}$, with half containing Ir11, Ir12 and Ir13 icosahedra and a Mg10 Frank–Kasper polyhedron with

we can conclude that the compound studied by the powder diffraction is fully ordered. Taking into account the single-crystal results we see that $Mg_{1+x}Ir_{1-x}$ shows a small homogeneity range between $x = 0$ and 0.054. The lattice parameters observed for single crystals and for the powder sample allow us to conclude the following about their anisotropic change with the magnesium content: *a*, *b* and cell volume increase, and *c* decreases, with increasing magnesium content. The difference between the single crystals (partly disordered) and the powder sample (fully ordered) reflects the difference in

Table 4
Selected bond distances (Å) for single crystal (1) of $Mg_{1+x}Ir_{1-x}$ (x = 0.037).

Ir1—Ir1	2.476 (1)	Ir6—Ir1	2.529 (1)
Ir1—M6	2.529 (1)	Ir6—Ir13	2.5879 (7)
Ir1—Ir12	2.5804 (8)	Ir6—Ir5	2.611 (1)
Ir1—Ir5	2.6365 (8)	Ir6—M2	2.625 (1)
Ir1—Mg4	2.777 (8)	Ir6—Ir4	2.646 (1)
Ir1—Mg1	2.799 (6)	Ir6—Mg3	2.823 (7)
Ir1—Mg9	2.857 (8)	Ir6—Mg1	2.848 (7)
Ir1—Mg12	2.91 (1)	Ir6—Mg5	2.853 (7)
Ir1—Mg11	2.975 (9)	Ir6—Mg11	2.912 (5)
Ir1—Mg6	3.011 (7)	Ir6—Mg10	2.936 (5)
Ir1—Mg12	3.023 (8)	Ir6—Mg7	2.971 (9)
Ir1—Mg10	3.04 (1)	Ir6—Mg6	3.115 (8)
Ir2—M2	2.560 (2)	Ir7—Ir8	2.452 (1)
Ir2—Ir8	2.590 (1)	Ir7—Mg12	2.57 (1)
Ir2—Ir11	2.617 (1)	Ir7—Ir3 × 2	2.588 (1)
Ir2—M6	2.625 (1)	Ir7—Mg3	2.898 (6)
Ir2—Ir4	2.654 (1)	Ir7—Mg3	2.898 (6)
Ir2—Mg2	2.820 (8)	Ir7—Mg11	2.918 (9)
Ir2—Mg3	2.881 (7)	Ir7—Mg1	2.931 (6)
Ir2—Mg7	2.950 (8)	Ir7—Mg1	2.931 (6)
Ir2—Mg10	2.952 (9)	Ir7—Mg10	3.188 (9)
Ir2—Mg11	3.020 (9)	Ir7—Mg4	3.368 (8)
Ir2—Mg8	3.021 (9)	Ir7—Mg4	3.368 (8)
Ir2—Mg8	3.07 (1)		
		Ir8—Ir7	2.452 (1)
Ir3—Ir4	2.4719 (8)	Ir8—M2 × 2	2.590 (1)
Ir3—Ir5	2.5077 (9)	Ir8—Mg9	2.61 (1)
Ir3—Ir7	2.588 (1)	Ir8—Mg3 × 2	2.909 (7)
Ir3—Ir3	2.646 (1)	Ir8—Mg11	3.00 (1)
Ir3—Mg9	2.855 (8)	Ir8—Mg2 × 2	3.069 (8)
Ir3—Mg1	2.927 (7)	Ir8—Mg4 × 2	3.155 (7)
Ir3—Mg2	2.939 (8)	Ir8—Mg8	3.29 (1)
Ir3—Mg5	2.967 (7)		
Ir3—Mg8	2.984 (9)	Ir9—Ir10	2.486 (2)
Ir3—Mg3	2.998 (7)	Ir9—Ir5 × 2	2.5015 (9)
Ir3—Mg10	3.048 (8)	Ir9—Mg2 × 2	2.726 (7)
Ir3—Mg11	3.142 (8)	Ir9—Mg5 × 2	2.898 (7)
		Ir9—Mg6 × 2	2.948 (7)
Ir4—Ir3	2.4719 (8)	Ir9—Mg4 × 2	3.060 (8)
Ir4—Ir11	2.6289 (8)		
Ir4—Ir13	2.6419 (7)	Ir10—Ir9	2.486 (2)
Ir4—M6	2.646 (1)	Ir10—Mg3 × 2	2.677 (7)
Ir4—M2	2.654 (1)	Ir10—Mg7 × 2	2.680 (7)
Ir4—Mg6	2.757 (7)	Ir10—Mg4 × 2	2.810 (7)
Ir4—Mg1	2.896 (8)	Ir10—Mg2 × 2	3.121 (7)
Ir4—Mg2	2.901 (7)	Ir10—Mg5 × 2	3.437 (8)
Ir4—Mg5	2.952 (7)		
Ir4—Mg7	2.952 (7)	Ir11—M2 × 2	2.617 (1)
Ir4—Mg10	2.979 (6)	Ir11—Ir4 × 2	2.6288 (8)
Ir4—Mg8	3.016 (6)	Ir11—Mg2 × 2	2.795 (7)
		Ir11—Mg7 × 2	2.829 (8)
Ir5—Ir9	2.5015 (9)	Ir11—Mg8 × 2	2.994 (5)
Ir5—Ir3	2.5077 (9)	Ir11—Mg6 × 2	3.141 (8)
Ir5—M6	2.611 (1)		
Ir5—Ir1	2.6365 (8)	Ir12—Ir1 × 2	2.5804 (8)
Ir5—Mg9	2.816 (5)	Ir12—Mg6 × 2	2.691 (5)
Ir5—Mg2	2.885 (7)	Ir12—Mg12 × 2	2.715 (5)
Ir5—Mg5	2.889 (7)	Ir12—Mg4 × 2	2.848 (7)
Ir5—Mg3	2.889 (8)	Ir12—Mg1 × 2	2.887 (8)
Ir5—Mg4	2.900 (8)	Ir12—Mg7 × 2	3.517 (8)
Ir5—Mg5	2.906 (7)		
Ir5—Mg11	3.039 (6)	Ir13—M6 × 2	2.5879 (7)
Ir5—Mg6	3.059 (7)	Ir13—Ir4 × 2	2.6420 (7)
		Ir13—Mg5 × 2	2.829 (6)
		Ir13—Mg1 × 2	2.886 (7)
		Ir13—Mg7 × 2	2.907 (8)
		Ir13— Mg6 ×2	2.929 (8)
Mg1—Ir1	2.799 (6)	Mg6—Ir12	2.691 (8)
Mg1—M6	2.848 (7)	Mg6—Ir4	2.757 (7)

Table 4 (continued)

Mg1—Ir13	2.886 (7)	Mg6—Mg5	2.88 (1)
Mg1—Ir12	2.887 (8)	Mg6—Ir13	2.929 (8)
Mg1—Ir4	2.896 (8)	Mg6—Ir9	2.948 (7)
Mg1—Mg10	2.91 (1)	Mg6—Mg4	2.96 (1)
Mg1—Ir3	2.927 (7)	Mg6—Mg7	2.99 (1)
Mg1—Ir7	2.931 (7)	Mg6—Ir1	3.011 (7)
Mg1—Mg7	2.98 (1)	Mg6—Ir5	3.059 (7)
Mg1—Mg12	3.00 (1)	Mg6—Mg2	3.11 (1)
Mg1—Mg4	3.03 (1)	Mg6—Ir6	3.115 (8)
Mg1—Mg5	3.08 (1)	Mg6—Ir11	3.141 (8)
Mg1—Mg6	3.261 (9)	Mg6—Mg7	3.21 (1)
Mg1—Mg3	3.424 (9)	Mg6—Mg1	3.261 (9)
Mg2—Ir9	2.726 (7)	Mg7—Ir10	2.680 (7)
Mg2—Ir11	2.795 (7)	Mg7—Ir11	2.829 (8)
Mg2—M2	2.820 (8)	Mg7—Ir13	2.907 (8)
Mg2—Ir5	2.885 (7)	Mg7—M2	2.950 (8)
Mg2—Ir4	2.901 (7)	Mg7—Ir4	2.952 (7)
Mg2—Mg4	2.917 (9)	Mg7—Ir6	2.971 (9)
Mg2—Ir3	2.939 (8)	Mg7—Mg1	2.98 (1)
Mg2—Mg8	2.972 (9)	Mg7—Mg6	2.99 (1)
Mg2—Mg7	3.01 (1)	Mg7—Mg2	3.01 (1)
Mg2—Ir8	3.069 (7)	Mg7—Mg5	3.04 (1)
Mg2—Mg9	3.112 (9)	Mg7—Mg3	3.16 (1)
Mg2—Mg6	3.11 (1)	Mg7—Mg6	3.21 (1)
Mg2—Ir10	3.121 (7)	Mg7—Mg4	3.25 (1)
Mg2—Mg3	3.42 (1)	Mg7—Ir12	3.517 (8)
Mg2—Mg5	3.73 (1)		
		Mg8—Mg2 × 2	2.972 (9)
Mg3—Ir10	2.677 (7)	Mg8—Ir3 × 2	2.984 (9)
Mg3—M6	2.823 (7)	Mg8—Ir11 × 2	2.993 (5)
Mg3—Ir2	2.881 (7)	Mg8—Ir4 × 2	3.016 (6)
Mg3—Ir5	2.889 (8)	Mg8—M2 × 2	3.021 (9)
Mg3—Ir7	2.898 (6)	Mg8—M2 × 2	3.07 (1)
Mg3—Ir8	2.909 (7)	Mg8—Mg10	3.07 (2)
Mg3—Mg4	2.93 (1)	Mg8—Mg8	3.11 (2)
Mg3—Mg11	2.929 (9)	Mg8—Ir8	3.29 (1)
Mg3—Mg5	2.95 (1)	Mg8—Mg9	3.31 (1)
Mg3—Ir3	2.998 (7)		
Mg3—Mg7	3.16 (1)	Mg9—Ir8	2.61 (1)
Mg3—Mg5	3.28 (1)	Mg9—Ir5 × 2	2.816 (5)
Mg3—Mg2	3.42 (1)	Mg9—Ir3 × 2	2.855 (8)
Mg3—Mg1	3.424 (9)	Mg9—Ir1 × 2	2.857 (8)
		Mg9—Mg11	2.87 (2)
Mg4—Ir1	2.777 (8)	Mg9—Mg4 × 2	3.077 (9)
Mg4—Ir10	2.810 (7)	Mg9—Mg2 × 2	3.112 (9)
Mg4—Ir12	2.848 (7)	Mg9—Mg8	3.31 (1)
Mg4—Ir5	2.900 (8)	Mg9—Mg12	3.55 (1)
Mg4—Mg2	2.917 (9)		
Mg4—Mg3	2.93 (1)	Mg10—Mg1 × 2	2.91 (1)
Mg4—Mg12	2.961 (9)	Mg10—M6 × 2	2.936 (5)
Mg4—Mg6	2.96 (1)	Mg10—M2 × 2	2.952 (9)
Mg4—Mg1	3.03 (1)	Mg10—Ir4 × 2	2.979 (6)
Mg4—Mg9	3.077 (9)	Mg10—Mg11	3.03 (1)
Mg4—Ir8	3.155 (7)	Mg10—Ir1 × 2	3.04 (1)
Mg4—Mg7	3.25 (1)	Mg10—Ir3 × 2	3.048 (8)
Mg4—Ir7	3.369 (8)	Mg10—Mg8	3.07 (2)
		Mg10—Ir7	3.188 (9)
Mg5—Ir13	2.829 (6)	Mg10—Mg12	3.59 (2)
Mg5—M6	2.853 (7)		
Mg5—Mg6	2.89 (1)	Mg11—Mg9	2.87 (2)
Mg5—Ir5	2.889 (7)	Mg11—M6 × 2	2.912 (4)
Mg5—Ir9	2.898 (8)	Mg11—Ir7	2.918 (9)
Mg5—Ir5	2.906 (7)	Mg11—Mg3 × 2	2.929 (9)
Mg5—Mg5	2.93 (1)	Mg11—Ir1 × 2	2.975 (9)
Mg5—Mg3	2.95 (1)	Mg11—Ir8	3.00 (1)
Mg5—Ir4	2.952 (7)	Mg11—M2 × 2	3.020 (9)
Mg5—Ir3	2.967 (7)	Mg11—Mg10	3.03 (1)
Mg5—Mg7	3.04 (1)	Mg11—Ir5 × 2	3.039 (6)
Mg5—Mg1	3.08 (1)	Mg11—Ir3 × 2	3.142 (8)
Mg5—Mg3	3.27 (1)		
Mg5—Ir10	3.437 (8)	Mg12—Ir7	2.57 (1)
		Mg12—Ir12 × 2	2.715 (5)

Table 4 (continued)

Mg5—Mg2	3.73 (1)	Mg12—Mg12	2.72 (2)
		Mg12—Ir1 × 2	2.91 (1)
		Mg12—Mg4 × 2	2.961 (9)
		Mg12—Mg1 × 2	3.00 (1)
		Mg12—Ir1 × 2	3.023 (8)
		Mg12—Mg9	3.55 (1)
		Mg12—Mg10	3.59 (2)

CN16, and (001) slabs at $z \simeq \frac{1}{4}$ and $\frac{3}{4}$ containing Ir5 and Ir8 icosahedra, and the Ir10 atom with a coordination polyhedron CN11 (see Fig. 2). This motif of condensation of various Frank–Kasper-related polyhedra is similar to that found in the structure of $Mg_{13}Ir_3$ (see Hlukhyy & Pöttgen, 2004a).

Other phases that are characterized in the Mg–Ir system ($Mg_{29}Ir_4$, $Mg_{44}Ir_7$, $Mg_{13}Ir_3$, Mg_3Ir and Mg_5Ir_2) are richer in magnesium, and have Ir and Mg atoms coordinated partly by Frank–Kasper polyhedra and partly by polyhedra with lower CN (9 or 10 for iridium and 13 for magnesium). The classification of $Mg_{1+x}Ir_{1-x}$ as a close-packed structure can also be justified from a comparison of the average volume per atom (in $Å^3$) observed in different phases of the Mg–Ir system: 16.5 for $Mg_{1+x}Ir_{1-x}$, 18.6 for Mg_5Ir_2, 18.4 for Mg_3Ir, 19.7 for $Mg_{13}Ir_3$, 19.9 for $Mg_{44}Ir_7$ and 29.6 for $Mg_{29}Ir_4$. The increase of the average volume per atom from $Mg_{1+x}Ir_{1-x}$ to $Mg_{29}Ir_4$ by 79.4% mainly reflects a decreasing packing efficiency, because the effect of increasing magnesium content is only 2.6%, as calculated from covalent radii.

No quasi-crystalline phase was reported in the Mg–Ir binary system, therefore, the hypothesis that $Mg_{1+x}Ir_{1-x}$, which is quite a complex crystal structure, is a crystalline approximant of an unknown quasicrystal was carefully considered. No symptoms such as the partial occupancy of many atomic sites or the existence of large atomic clusters in the crystal structure were, however, observed.

3.5. Interatomic distances (based on the single-crystal data)

The interatomic distances Ir–Ir in $Mg_{1+x}Ir_{1-x}$ cover the range from 2.45 to 2.66 Å, and, to the best of our knowledge, are the shortest ones ever observed. These Ir—Ir contacts are significantly shorter than the sum of the covalent radii for two Ir atoms (2.54 Å; Emsley, 1999) and than the distances in *f.c.c.* (face-centered cubic) iridium (2.72 Å; Donohue, 1974). We can assume significant Ir–Ir bonding in the MgIr structure. In comparison, the Ir—Ir distance in a compound with an equiatomic composition (LiIr; Donkersloot & Van Vucht, 1976) is 2.65 Å. The short Ir—Ir distances identified in $Mg_{1+x}Ir_{1-x}$ are also shorter than those usually observed in iridium cluster compounds (2.63–2.73 Å).

The Mg—Mg distances in MgIr are in the range 2.85–3.73 Å. Most of the Mg—Mg distances are shorter than the average Mg—Mg distance of 3.20 Å in *h.c.p.* (hexagonal close packed) magnesium (Donohue, 1974). However, similar short Mg—Mg distances also occur in other transition metal magnesium compounds, *e.g.* Pd_2Mg_5 (2.95 Å; Hlukhyy & Pöttgen, 2004b).

The Mg—Ir distances in $Mg_{1+x}Ir_{1-x}$ are in the range 2.57–3.51 Å. The shorter Ir—Mg distances are shorter than the sum of the covalent radii of 2.63 Å (Emsley, 1999) and correspond well to the range of observed distances in other compounds in this system: 2.62–3.12 Å. Considering the range of the interatomic distances, we can assume more or less isotropic and strong bonding within this peculiar structure.

4. Conclusions

$Mg_{1+x}Ir_{1-x}$ is a topologically close-packed phase virtually compliant with the definition of Frank–Kasper phases. The coordination of nearly all the atoms is in the form of Frank–Kasper polyhedra, with the exception of two Ir atoms. The compound contains 13 Ir and 12 Mg atoms in the asymmetric unit, shows a small homogeneity range at higher temperatures and was fully structurally characterized on separate samples by synchrotron powder and single-crystal X-ray diffraction. The compound contains the shortest Ir—Ir distances ever observed and also very short Mg—Mg distances, both are close to or shorter than the sum of the corresponding covalent radii.

The global optimization method of structural solution from powder diffraction was successfully applied here on a 25-atom structure with close packing and high symmetry, where methods using extracted integrated intensities from the powder pattern (direct methods or Patterson synthesis) failed, probably because of the difficult recognition of a structural motif either in E- or Patterson maps.

References

Bérar, J.-F. & Lelann, P. (1991). *J. Appl. Cryst.* **24**, 1–5.
Bonhomme, F. & Yvon, K. (1995). *J. Alloys Comput.* **227**, L1–L3.
Boultif, A. & Louër, D. (1991). *J. Appl. Cryst.* **24**, 987–993.
Černý, R., Joubert, J.-M., Kohlmann, H. & Yvon, K. (2002). *J. Alloys Comput.* **340**, 180–188.
Compton, V. B. (1958). *Acta Cryst.* **11**, 446.
David, W. I. F. (1999). *J. Appl. Cryst.* **32**, 654–663.
Donkersloot, H. C. & Van Vucht, J. H. N. (1976). *J. Less-Common Met.* **50**, 279–282.

Donohue, J. (1974). *The Structures of the Elements*. New York: Wiley.

Emsley, J. (1999). *The Elements*. Oxford University Press.

Favre-Nicolin, V. & Černý, R. (2002). *J. Appl. Cryst.* **35**, 734–743.

Ferro, R. (1959). *J. Less-Common Met.* **1**, 424–438.

Ferro, R., Rombaldi, G. & Capelli, C. (1962). *J. Less-Common Met.* **4**, 16–23.

Frank, F. C. & Kasper, J. C. (1958). *Acta Cryst.* **11**, 184–190.

Frank, F. C. & Kasper, J. C. (1959). *Acta Cryst.* **12**, 483–499.

Hill, R. J. & Flack, H. D. (1987). *J. Appl. Cryst.* **20**, 356–361.

Hlukhyy, V., Hoffmann, R.-D. & Pöttgen, R. (2004a). *Intermetallics*, **12**, 383–387.

Hlukhyy, V., Hoffmann, R.-D. & Pöttgen, R. (2004b). *Z. Anorg. Allg. Chem.* **630**, 68–74.

Hlukhyy, V. & Pöttgen, R. (2004a). *J. Solid State Chem.* **177**, 1646–1650.

Hlukhyy, V. & Pöttgen, R. (2004b). *Intermetallics*, **12**, 533–537.

Hlukhyy, V., Rodewald, U. ch., Hoffmann, R.-D. & Pöttgen, R. (2004). *Z. Naturforsch. B*, **59**, 251–255.

Kohlmann, H. (1999). Personal communication.

Kußmann, D., Hoffmann, R.-D. & Pöttgen, R. (1998). *Z. Anorg. Allg. Chem.* **624**, 1727–1735.

Massalski, T. B., Okamoto, H., Subramanian, P. R. & Kacprzak, L. (1996). Editors. *Binary Alloy Phase Diagrams*, 2nd ed., Version 1.0. NewYork: ASM International.

Pawley, G. S. (1980). *J. Appl. Cryst.* **13**, 630–633.

Pearson, W. B. (1967). *A Handbook of Lattice Spacings and Structures of Metals and Alloys*, Vol. 2, p. 1. Oxford: Pergamon Press.

Pöttgen, R., Gulden, Th. & Simon, A. (1999). *GIT Labor-Fachzeitschrift*, **43**, 133–136.

Range, K. J. & Hafner, P. (1993). *J. Alloys Comput.* **191**, L5–L7.

Rodríguez-Carvajal, J. (2002). *Program FullProf.2k*, Version 2.20. Laboratoire Léon Brillouin (CEA–CNRS), France.

Sheldrick, G. M. (1997a). *SHELXS*97. University of Göttingen, Germany.

Sheldrick, G. M. (1997b). *SHELXL*97. University of Göttingen, Germany.

Yoshida, M., Bonhomme, F. & Yvon, K. (1993). *J. Alloys Comput.* **190**, L45–L46.

Yvon, K., Jeitschko, W. & Parthé, E. (1977). *J. Appl. Cryst.* **10**, 73–74.

Westin, L. (1971). *Chemica Scr.* **1**, 127.